14th Congress of the International Society for Photogrammetry

Hamburg 1980

Commission No. V
Working Group No. 6

Presented Paper

HOLOGRAPHIC NUMERICAL ANALYSIS IN BIOSTEREOMETRICS

by

Ryszard J. Pryputniewicz
Department of Mechanical Engineering
Worcester Polytechnic Institute
Worcester, Massachusetts 01609
U. S. A.

## ABSTRACT

To effectively correct skeletal disharmonies, by application of external forces, the knowledge of the relationship between the applied force system and the resulting epiphyseal, bony, and sutural remodeling, influenced by muscle response, is necessary. Recent advances in holographic numerical analysis allow accurate quantification of these processes. In this paper, a new, non-invasive method for holographic determination of bone motions, in three-dimensional space, is presented and its use in studies of skull bone displacements and in orthodontics is discussed.

## Introduction

Modern treatment of skeletal disharmonies and malocclusions utilizes the application of external forces. In order to effectively use these therapeutic forces, mapping of three-dimensional displacements of bones with correlation to biological changes is required. In the past, this problem has been studied in a number of ways, using, for example, strain gauges, brittle coatings, photoelasticity, as well as clinical observations and mathematical modeling [1]. Because of their inherent limitations, these techniques did not always provide all the information necessary for development of meaningful relationships between the applied force system and the resulting periodontal, bony, or sutural remodeling. However, recent advances in the field of hologram interferometry allowed to circumvent some of these difficulties and permitted development of a new technique for non-invasive quantification of bone motions in three-dimensional space [2, 3].

Holography can be defined as a process in which, first, the optical information about an object is collected and stored within a suitable medium and, later, the information is retrieved from this medium and made visible in the form of an image. Out of the variety of the existing holographic procedures [4], the most suitable technique for biostereometric applications is the double-exposure method. In this method, two consecutive positions of an object are recorded in the same photographic emulsion; the object being displaced and/or deformed (by application of a force) between the two exposures. Upon reconstruction of the hologram, two three-dimensional images of the object are formed. Since both images appear in coherent (laser) light and exist in approximately the same location in space, they interfere with each other and produce fringes overlying the reconstructed image. All information about the object's motion is stored in this fringe pattern. Obviously, a unique deformation of an object, for a given illumination and observation geometry, does produce a unique three-dimensional interferogram, within a hologram reconstruction, from which the vectorial motion of the object can be determined.

Holographic techniques are particularly useful in biostereometrics because they are non-invasive, and provide rapid and accurate, three-dimensional mapping of displacements over the entire surface of the investigated object, as, for example, shown in Fig. 1. As such, they have already been used in studies of displacements of human teeth [5-8], as well as in investigations of skull bone displacements [9, 10] resulting from external loads.

Recent developments in the field of hologram interferometry [11] allowed further improvement in the currently used procedures and extended their utility in biostereometric applications. In this paper, the new general relationships for determination of vectorial displacements directly from holograms are presented and their use in representative biostereometric applications is outlined.

## Theory

In biostereometrics, one often desires to investigate objects for which the entire surface has moved and/or deformed. In such applications, it is rather difficult to determine true fringe orders and, therefore, conventional procedures of hologram interferometry do not apply. Instead,

R. J. Pryputniewicz (V-6)

we may only determine fringe order number for the point on the object, chosen for the origin of the coordinate system, to within an additive constant. Let us call this additive constant $\Omega_O$ and let us bear in mind that it comes from the lack of knowledge of the absolute fringe order.

Usual methods of holographic displacement analysis eliminate the unknown $\Omega_O$ from the system of equations by subtracting one member of the set from the rest, or by subtracting pairs of equations [12, 13]. However, in the subtraction process, the effects of some measurement errors can be escalated [14]. Nevertheless, we should note that in the case when the first observation is made through a point lying within the center of all points through which observations are made, it does not matter whether we introduce the additive constant $\Omega_O$ or simply use fringe shifts alone as discussed in References 12 and 13. The result will be the same. It is in the case when we want to make observations in an arbitrary fashion, with the first observation not being through the central point, that $\Omega_O$ must be employed; use of the other approach will give erratic results.

In holographic analysis, the scalar product of object's vectorial displacement $\underline{L}$ with the sensitivity vector $\underline{K}$ is related to the fringe order number n by the equation

$$ \mathbf{K} \cdot \mathbf{L} = 2\pi n = \Omega , \qquad (1) $$

where $\Omega$ is the fringe-locus function, constant values of which define fringe loci on the surface of the object. The sensitivity vector $\underline{K}$, appearing in Eq. 1, is defined as a difference between the observation vector $\underline{K}_2$ and the illumination vector $\underline{K}_1$ (see Fig. 2), that is,

$$ \mathbf{K} = \mathbf{K}_2 - \mathbf{K}_1 . \qquad (2) $$

Therefore, for each observation of a holographically reconstructed image we can write an equation of the type of Eq. 1, relating the observation-illumination geometry and fringe orders to the unknown object displacement. Generally, four observations are required in order to determine the vectorial motion of the object and the additive constant $\Omega_O$. However, it is common in holographic analysis to use more than four observations in order to reduce experimental errors. In cases such as this, one solves for the four parameters that yield the least-square-error in an attempt to satisfy the overdetermined set of equations that is generated from the excess data.

Let us assume that we successfully recorded a double-exposure hologram of an object that has experienced some kind of a motion between the two exposures. The hologram was processed and, now, we make multiple observations of the fringe pattern, seen within the hologram reconstruction, as shown in Fig. 2. If the first observation is made along direction $\underline{K}_2^1$ through some arbitrary point on the hologram, then, we can write an equation relating the arbitrary constant $\Omega_O$ to the scalar product of the unknown object displacement $\underline{L}$ with the sensitivity vector $\underline{K}^1$, corresponding to this first observation, as

$$ \mathbf{K}^1 \cdot \mathbf{L} = \Omega^1 = \Omega_o , \qquad (3) $$

where, according to Eq. 2,

$$ \mathbf{K}^1 = \mathbf{K}_2^1 - \mathbf{K}_1 . \qquad (4) $$

Next, the view is changed from observation along $\underline{K}_2^1$ direction to that along $\underline{K}_2^2$ direction. During this change, while continuously observing the object,

we count the fringes that pass across the point of interest on the object. In this way, we determine the observed fringe order, more commonly known as the fringe shift, $n^{1,2}$, which relates to the change $\Delta\Omega^{1,2}$ in the fringe-locus function via

$$\Delta\Omega^{1,2} = 2\pi n^{1,2} , \tag{5}$$

thus giving

$$\mathbf{K}^2 \cdot \mathbf{L} = \Omega^2 = \Omega_o + \Delta\Omega^{1,2}. \tag{6}$$

Following the same procedure, we may determine the fringe shifts $n^{1,m}$ for other changes in observation from the $\underset{\sim}{K}_2^1$ direction to the $\underset{\sim}{K}_2^m$ direction and, in general, we may write equivalents of Eqs 4 to 6 as

$$\mathbf{K}^m = \mathbf{K}_2^m - \mathbf{K}_1 , \tag{7}$$

$$\Delta\Omega^{1,m} = 2\pi n^{1,m} , \tag{8}$$

and

$$\mathbf{K}^m \cdot \mathbf{L} = \Omega^m = \Omega_o + \Delta\Omega^{1,m} , \tag{9}$$

respectively, where $m = 1, 2, \ldots, r$, with r being the total number of observations. We should note, that for $m = 1$ Eq. 7 is equal to Eq. 4, Eq. 8 gives $\Delta\Omega^{1,1} = 0$, and, finally, Eq. 9 yields Eq. 3. In this approach, however, r has to be equal to or be larger than four (that is $r \geq 4$) because in addition to the three unknown components of the displacement vector $\underset{=}{L}$ we must also account for $\Omega_o$ which is also an unknown. Therefore, from Eq. 9, we have

$$\mathbf{K}^m \cdot \mathbf{L} - \Omega_o = \Delta\Omega^{1,m} , \quad m = 1, 2, \ldots, r . \tag{10}$$

Since $\underset{=}{L}$ and $\Omega_o$ are common to all r equations, the set of equations given by Eq. 10 can be combined into a single matrix equation

$$\begin{bmatrix} \underset{\sim}{K}, & -1 \end{bmatrix} \begin{pmatrix} \mathbf{L} \\ \Omega_o \end{pmatrix} = \Delta\mathbf{\Omega} , \tag{11}$$

where $[\underset{\sim}{K}, -1]$ is a rectangular r x 4 matrix, $\begin{pmatrix} \underset{=}{L} \\ \Omega_o \end{pmatrix}$ is a column 4 x 1 matrix, and $(\Delta\underset{=}{\Omega})$ is a column r x 1 matrix. Defining the $[\underset{\sim}{K}, -1]$ matrix of sensitivity vectors as $\underset{\sim}{G}$, that is,

$$\begin{bmatrix} \underset{\sim}{K}, & -1 \end{bmatrix} = \underset{\sim}{G} , \tag{12}$$

we can write Eq. 11 as

$$\underset{\sim}{G} \begin{pmatrix} \mathbf{L} \\ \Omega_o \end{pmatrix} = \Delta\mathbf{\Omega} . \tag{13}$$

Finally, solving Eq. 13 we obtain

$$\begin{pmatrix} \mathbf{L} \\ \Omega_o \end{pmatrix} = \begin{bmatrix} \underset{\sim}{G}^T \underset{\sim}{G} \end{bmatrix}^{-1} \begin{pmatrix} \underset{\sim}{G}^T \Delta\mathbf{\Omega} \end{pmatrix} , \tag{14}$$

where $\Omega_o$ is equivalent to the fringe order that would have been assigned to the fringe passing the point of interest on the object, while observing it along the direction $\underset{\sim}{K}_2^1$, had the zero order fringe been identifiable.

R. J. Pryputniewicz (V-6)

The displacement $\underline{L}$ computed from Eq. 14 represents total motion of the object under investigation. This total motion results from a superposition of both, object motions induced by the applied external force (e. g., tooth motion due to orthodontic forces) and the natural motions (e. g., gross head motion). Therefore, in order to develop meaningful relationships between the applied force system and the resulting biomedical remodeling, we have to be able to account for both of these motions. This can be done by resolving the motion $\underline{L}_i$ at any point i on the object into corresponding bulk body translation $\underline{L}_o$ and rotation $\underline{\theta}$ [2], that is,

$$\mathbf{L}_i = \mathbf{L}_o + \mathbf{R}_i \times \mathbf{\Theta} , \qquad i = 1, 2, ..., q \tag{15}$$

In Eq. 15, q denotes the total number of object points considered in calculations, and $\underline{R}_i$ is the space vactor, from the origin of an arbitrarily chosen coordinate system to the ith point on the object, defined as

$$\mathbf{R}_i = x_i \hat{i} + y_i \hat{j} + z_i \hat{k} , \quad i = 1, 2, ..., q \tag{16}$$

with $x_i$, $y_i$, and $z_i$ being components of $\underline{R}_i$ in directions of the unit vectors $\hat{i}$, $\hat{j}$, and $\hat{k}$ of the Cartesian coordinate system, respectively.

The set of q equations given by Eq. 16 may be written in a matrix form as

$$(\mathbf{L}_i) = \begin{bmatrix} \underset{\sim}{I} & \underset{\sim}{R}_i \end{bmatrix} \begin{pmatrix} \mathbf{L}_o \\ \mathbf{\Theta} \end{pmatrix} , \quad i = 1, 2, ..., q , \tag{17}$$

and solved [2] to obtain

$$\begin{pmatrix} \mathbf{L}_o \\ \mathbf{\Theta} \end{pmatrix} = \underset{\sim}{\xi}^{-1} \underset{\approx}{\Xi}^T \mathbf{L}_i , \quad i = 1, 2, ..., q , \tag{18}$$

where

$$\underset{\approx}{\Xi} = \begin{bmatrix} \underset{\sim}{I} & \underset{\sim}{R}_i \end{bmatrix} , \quad i = 1, 2, ..., q , \tag{19}$$

$$\underset{\sim}{\xi} = \underset{\approx}{\Xi}^T \underset{\approx}{\Xi} , \tag{20}$$

$\underset{\sim}{I}$ is the 3 × 3 identity matrix, and $\underset{\sim}{R}_i$ is the a 3 × 3 antisymmetric matrix corresponding to the space vector $\underline{R}_i$ defined in Eq. 16.

Using Eq. 18 and considering three or more points on the object that experienced rigid-body motion (that is, q≥3) the 6 × 1 matrix $\begin{pmatrix} \underline{L}_o \\ \underline{\theta} \end{pmatrix}$ of corresponding translations and rotations can be determined from $\underline{\theta}$ holograms. If we are also able to determine total translation $\underline{L}_P$ and rotation $\underline{\theta}_P$ at a point P on the studied object (see Fig. 3), using, for example, procedures developed in References 12 and 15, then we can determine motions $\underline{L}_{P_{rel}}$ and $\underline{\theta}_{P_{rel}}$ of this point P relative to the rest of the object [2]. In order to do so, we must first determine the rigid-body translation $\underline{L}_{P_{rig}}$ at the point P on the object, defined by a space vector $\underline{R}_P$ as shown in Fig. 3, because translations are position dependent. Therefore, using an equivalent of Eq. 17, we determine rigid-body translation at point P, that is,

$$\mathbf{L}_{P_{rig}} = \begin{bmatrix} \underset{\sim}{I} & \underset{\sim}{R}_P \end{bmatrix} \begin{pmatrix} \mathbf{L}_o \\ \mathbf{\Theta} \end{pmatrix} , \tag{21}$$

where $\underline{L}_o$ and $\underline{\theta}$ have values determined from Eq. 18 and $\underline{R}_P$ is a 3 × 3 antisymmetric matrix defining the space vector $\underline{R}_P$, from the origin of the coordinate system to the point of interest on the object. Next, we subtract the $\underline{L}_{P_{rig}}$ from the total translation $\underline{L}_P$ to obtain $\underline{L}_{P_{rel}}$, thus,

R. J. Pryputniewicz (V-6)

$$L_{P_{rel}} = L_P - L_{P_{rig}} \quad . \tag{22}$$

Noting that the rigid-body rotations are independent of the position on the surface of the object we subtract $\underline{\theta}$ (computed from Eq. 18) directly from total rotations $\underline{\theta}_P$ to obtain

$$\Theta_{P_{rel}} = \Theta_P - \Theta \quad . \tag{23}$$

Equations 22 and 23 allow determination of translations and rotations at any point on the object relative to the rest of the body.


## Representative applications

The procedure described in this paper, is particularly useful in studies of orthodontic tooth movement and in determination of displacements of skull bones.  In the following, we will examine two examples relating to the above problems.

Let us first consider application of the method in the case where we wish to determine motions of a point on the maxillary central incisor, defined by a space vector $\underline{R}_P$, and loaded in some arbitrary fashion as shown in Fig. 3.  In order to obtain desired results we have to solve Eq. 18 by choosing three or more points on the maxilla.  Let us assume that we have decided to compute translations and rotations of the patient's head based on motions of points defined by space vectors $\underline{R}_1$, $\underline{R}_2$, and $R_3$ and located on the right and left cuspids and the first molar, respectively; these three teeth are not subjected to the applied force system and as such undergo only rigid-body motion, if any, that might take place while recording holograms. Then, solution of Eq. 18 will result in the components of vectors $\underline{L}_0$ and $\underline{\theta}$.

Providing we can determine displacement Lp, Eq. 21 can be used to determine rigid-body translation of point P at a known $\underline{R}_P$ on the maxillary central incisor.  Finally, from Eq. 22 we can compute $\underline{L}_{P_{rel}}$, and with known $\underline{\theta}_P$ we can compute $\underline{\theta}_{P_{rel}}$ from Eq. 23.  Vectors $\underline{L}_{P_{rel}}$ relate directly to the applied force system.

As the second example, let us consider a problem of determining relative motions of skull bones resulting from a force applied, for example, at the maxilla (see Fig. 4).  In particular, we are interested in translations and rotations of the zygometic, frontal, and parietal bones.

From a holographic image, we can easily determine motions at various points on the skull, using Eq. 14.  Let us say, that points 1 to 3 are located on the zygomatic bone, points 4 to 6 are on the frontal bone, whereas points 7 through 10 are on the parietal bone, as shown in Fig. 14.  Then, space vectors $\underline{R}_1$ to $\underline{R}_3$ together with the corresponding displacements are used to compute, from Eq. 18, the translations $\underline{L}_{0z}$ and rotations $\underline{\theta}_z$ of the zygomatic bone.  Next, $\underline{L}_{0f}$ and $\underline{\theta}_f$ as well as $\underline{L}_{0p}$ and $\underline{\theta}_p$ are computed in a similar way for the frontal and parietal bones, respectively.  Since all of these translations and rotations are determined with respect to the origin of the same coordinate system, simple vectorial subtraction will give us relative vectorial motions of the bones.

The above procedure may be extended to determine sutural deformations. This can be explained by considering relative displacement of points a

R. J. Pryputniewicz (V-6)

and b located on the edges of the coronal suture, shown in Fig. 4. These points are defined by space vectors $\underline{R}_a$ and $\underline{R}_b$ with respect to the same x-y-z coordinate system as used in previous calculations. Then, using Eq. 21 we obtain

$$L_{a_{rig}} = \begin{bmatrix} \underset{\sim}{I} & \underset{\sim}{R}_a \end{bmatrix} \begin{pmatrix} L_{o_f} \\ \Theta_f \end{pmatrix}, \qquad (24)$$

and

$$L_{b_{rig}} = \begin{bmatrix} \underset{\sim}{I} & \underset{\sim}{R}_b \end{bmatrix} \begin{pmatrix} L_{o_p} \\ \Theta_p \end{pmatrix}. \qquad (25)$$

Finally, using Eq. 22, we compute the relative motion $\underline{L}_{ab_{rel}}$ to be

$$L_{ab_{rel}} = L_{a_{rig}} - L_{b_{rig}}. \qquad (26)$$

In a similar manner, bone displacements and relative motions at other points on the skull can be determined and correlated with the applied force system.

## Conclusions

The method for holographic determination of displacements, presented in this paper, allows for accurate, non-invasive quantification of bone motions in three-dimensional space. The necessary parameters are obtained directly from multiple observations of holographically reconstructed images and the governing equations are solved, for numerical values of vectorial displacements, as discussed herein. The use of the technique for measurement purposes was briefly described by way of examples, which also show possible ways of extending the current technique to other biostereometric applications.

## References

1. R. J. Isaacson and C. J. Burstone, "Malocclusion in bioengineering," in The Relevence of Biomedical Engineering to Dentistry, E. Attinger and P. Parakkal, ed's, DHEW Pub. No. (NIH) 77-1198 (1976).

2. R. J. Pryputniewicz, "Holographic determination of rigid-body motions and application of the method to orthodontics," Appl. Opt., 18:1442 (1979).

3. R. J. Pryputniewicz and C. J. Burstone, "The effect of time and force magnitude on orthodontic tooth movement," J. Dent. Res., 58:1754 (1979).

4. R. J. Pryputniewicz, Laser Holography, Worcester Polytechnic Institute, Worcester, MA (1979).

5. P. R. Wedendal and H. I Bjelkhagen, "Dynamics of human teeth in function by means of double pulsed holography - an experimental investigation," Appl. Opt., 13:2481 (1974).

6. C. J. Burstone, R. J. Pryputniewicz, and W. W. Bowley, "Incisor tooth displacement in the human," J. Dent. Res., 55B:104 (1976).

7. C. J. Burstone, R. J. Pryputniewicz, and W. W. Bowley, "Holographic measurement of tooth mobility in three dimensions," J. Periodontal

Res., 13:283 (1978).

8.  R. J. Pryputniewicz and C. J. Burstone, "Primary centers of rotation in human teeth," J. Dent. Res., 58A:402 (1979).

9.  C. C. Sapp, R. J. Pryputniewicz, and R. Nanda, "Skull bone displacements generated by extraoral forces," J. Dent. Res., 58A:374 (1979).

10. G. Kragt, J. J. Ten Bosch, and P. C. F. Borsboom, "Measurement of bone displacement in a macerated human skull induced by orthodontic forces; a holographic study," J. Biomech., 12:905 (1979).

11. R. J. Pryputniewicz and K. A. Stetson, "Fundamentals and applications of laser speckle and hologram interferometry," Worcester Polytechnic Institute, Worcester, MA (1980).

12. R. J. Pryputniewicz and W. W. Bowley, "Techniques of holographic displacement measurement: an experimental comparison," Appl. Opt., 17: 1748 (1978).

13. C. M. Vest, Holographic Interferometry, Wiley, New York (1979).

14. K. A. Stetson, private communication.

15. R. J. Pryputniewicz and K. A. Stetson, "Holographic strain analysis: extension of fringe-vector method to include perspective," Appl. Opt., 15:725 (1976).
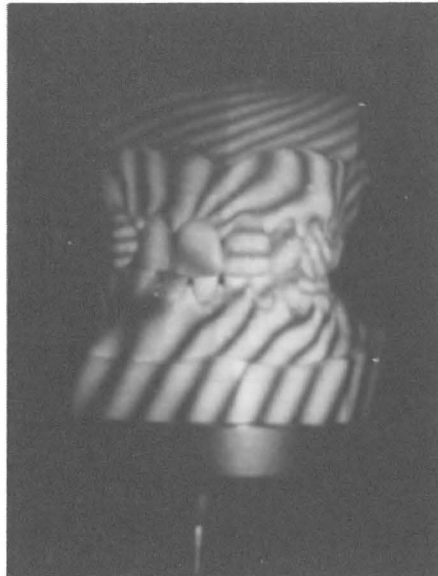
Fig. 1. A photograph of holographically reconstructed image of a typodont loaded with a vertical force applied at the maxilla. Note different fringe patterns on individual teeth, corresponding to their arbitrary displacements.
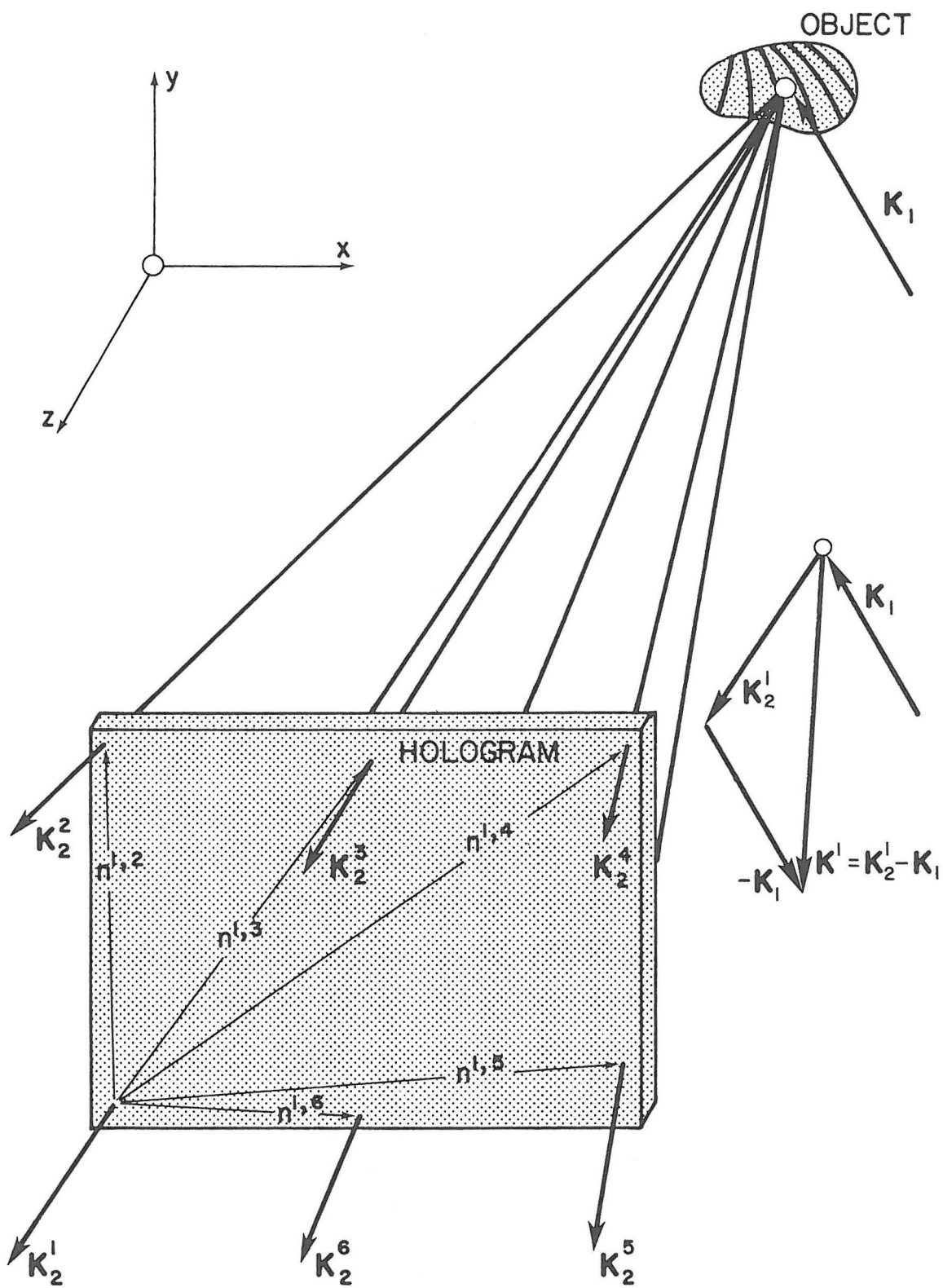
Fig. 2. Observation geometry in hologram interferometry.

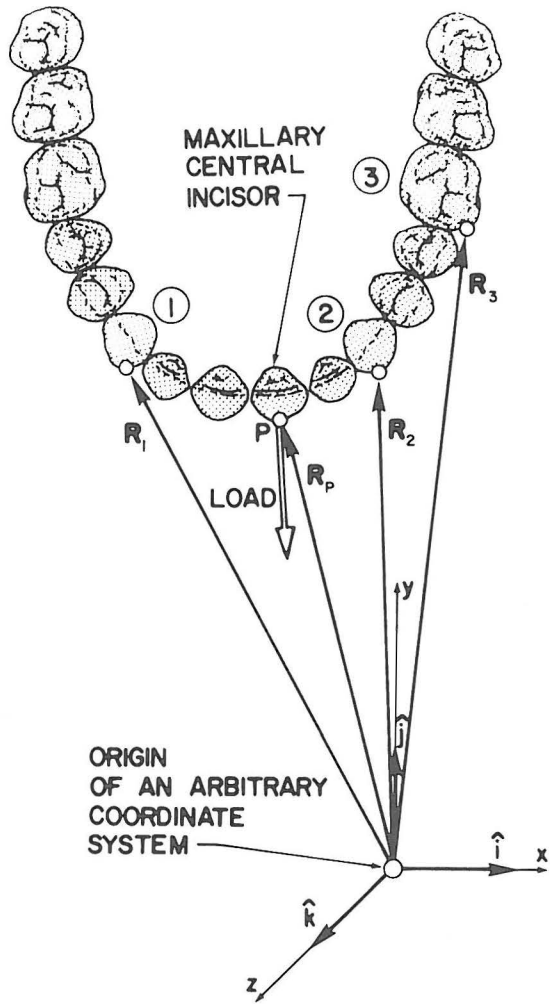R. J. Pryputniewicz (V-6)

Fig. 3. Geometry for holographic determination of rigid-body motions in orthodontic tooth displacement studies.
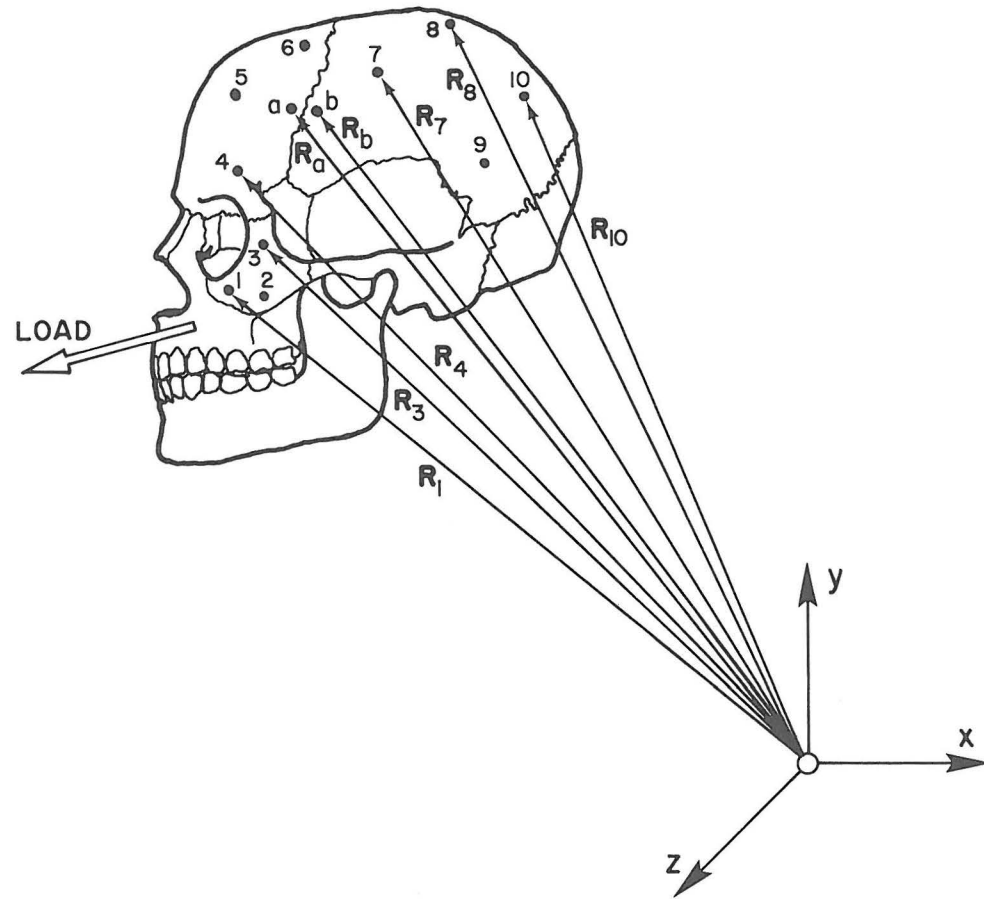


Fig. 4. Geometry for holographic determination of relative motions of skull bones. In this figure, some of the space vectors were omitted for clarity.

R. J. Pryputniewicz (V-6)